

Numerical simulation of flow past a bluff body of two different shapes using gradient smoothing method with unstructured grids

Da Hui^a, Guiyong Zhang^{a,b,c,*}, Jianyao Yao^d, A-Man Zhang^e, Shuangqiang Wang^a, Zhi Zong^{a,b,c}

^a Liaoning Engineering Laboratory for Deep-Sea Floating Structures, School of Naval Architecture, Dalian University of Technology, Dalian 116024, PR China

^b State Key Laboratory of Structural Analysis for Industrial Equipment, Dalian University of Technology, Dalian 116024, PR China

^c Collaborative Innovation Center for Advanced Ship and Deep-Sea Exploration, Shanghai, 200240, PR China

^d College of Aerospace Engineering, Chongqing University, Chongqing 400044, PR China

^e College of Shipbuilding Engineering, Harbin Engineering University, Harbin 150001, PR China

ARTICLE INFO

Keywords:

Gradient smoothing method
Triangular cylinder
Circular cylinder
Strouhal number
Drag and lift coefficient

ABSTRACT

In this paper, flow across a bluff cylinder with circular and equilateral triangular sections shapes at low Reynolds number ($10 \leq Re \leq 250$) is numerically investigated using the gradient smoothed method (GSM). The method was originally developed based on unstructured grids, which could be generated easily for complicated domains. For solving the incompressible flow, artificial compressibility terms are introduced in Navier–Stokes equations. The spatial derivatives of convective and viscous fluxes are obtained using the gradient smoothing operation. And the time marching is implemented based on the dual time stepping technique. The situations of steady flows with $Re = 10\text{--}40$ and unsteady flows with $Re = 50\text{--}250$ are simulated. Analysis of the drag coefficients, root mean square (rms) value of lift coefficients and Strouhal number of circular and triangular cylinders has been carried out. Compared with both experimental and numerical reference solutions in the literatures, the accuracy of GSM results has been demonstrated.

1. Introduction

Generalized smoothing technique has been extensively used for solving various physical problems after decades of development [1–5]. Based on strain smoothing technique, the smoothing finite element method (S-FEM) has been proposed. S-FEM has been applied to solve not only solid mechanics [6–8] but also acoustic [9–11] and heat transfer problems [12,13]. And the bubble function was introduced to further improve numerical stability [14–16]. The numerical solution can satisfy the divergence-free conditions. For hydromechanics, gradient smoothing technique has been extended to directly perform in the strong form formulation (Navier–Stokes equation) and such method is named as the gradient smoothing method (GSM) [17]. GSM has been used to solve the general hydrodynamic flows [18], biomechanics [19,20] and fluid-structure interactions [21,22]. Intensive numerical tests have demonstrated that GSM can provide accurate, efficient and robust solutions, which is insensitive to mesh distortions. Thus, it would be interesting to further develop the GSM to simulate flow past a bluff body which is a classical hydrodynamics.

In the framework of GSM, field variables are located at the vertices of the background grids. The spatial derivatives can be approximated based on gradient smoothing operations [17]. And different kinds

smoothing functions and quadrature schemes can be chosen for approximating the first and second order derivatives. This can offer efficient, stable and accurate solutions by properly choosing the smoothing functions and quadrature schemes on even highly distorted unstructured grids [18].

Recently, most of the research efforts with GSM have been widely developed for different fluid flow problems. The GSM solution of incompressible flows problems is achieved using the artificial compressibility method [23]. And by incorporating the arbitrary Lagrangian–Eulerian (ALE) moving-mesh technique, fluid-structure interaction (FSI) problem can be solved [24]. By using adaptive grid technique, a high computational efficiency is obtained in GSM. The adaptive GSM was also developed to yield a set of optimal grids so that accurate results can be obtained using locally refined grid [2]. Based on previous research, GSM was further extended to solve three dimensions problems [25].

The main purpose of this work is to numerically study the flow around a bluff body at low Reynolds number using unstructured grids. Flow past bluff bodies has been the major concern in engineering, such as flow metering devices, structural design and acoustic emission. Thus it has been extensively studied with considerable experimental and numerical investigations. At very low Reynolds number, it is observed that the flow is symmetric and steady. And there is no separation occurring at

* Corresponding author at: State Key Laboratory of Structural Analysis for Industrial Equipment, Dalian University of Technology, Dalian 116024, PR China.
E-mail address: ldgyzhang@dut.edu.cn (G. Zhang).

the surface of body. With the increasing of Reynolds number, the vortex shedding periodically from the body causes the instability of wake. Particularly, this work will be dealing with the steady and unsteady wake behind the bluff body with different shapes, especially, the periodic drag coefficient and vortex shedding, which are also the interests of most of research [26–30]. And many experiment studies have investigated the steady and unsteady behaviors in the wake [31–34].

While, for numerical simulation, the previous research works on flow around a bluff body have used structured grids [35–37]. For complex shape domains, the structured grids generation is a larger burden in computational process. However, the unstructured grids can work with greater efficiency and more flexibility. Thus, the unstructured triangular grids in hydrodynamics are widely used in practical engineering. Coincidentally, the previous research efforts repeatedly demonstrated that the GSM solution with unstructured triangular grids is stable and accurate [17,18,38]. Thus GSM provides a good choice of solving the problem using unstructured grids. In addition, the hydrodynamic behavior of flow past both circular and triangular cylinder is also exhibited and compared.

In this paper, the Navier–Stokes equations are introduced in Section 2. The artificial compressibility terms are added for solving the incompressible flow. Then in Section 3, a brief introduction of the principle of the GSM is provided. And the numerical method and boundary condition are given. Section 4 presents the numerical results of reattachment length for steady solution. The Strouhal number and drag coefficients for unsteady solution are presented. This study visualizes steady and unsteady flow field. These results are obtained with the proposed GSM with Reynolds number varying from 10 to 250 and have been compared with experimental measurements and other numerical results in great detail. Some conclusions are derived in Section 5.

2. Mathematical formulation

Two-dimensional incompressible Navier–Stokes equations in Cartesian coordinate are written as follows [18]

$$\begin{aligned} \frac{\partial v_x}{\partial x} + \frac{\partial v_y}{\partial y} &= 0 \\ \frac{\partial \rho v_x}{\partial t} + \frac{\partial(\rho v_x^2 + p)}{\partial x} + \frac{\partial \rho v_x v_y}{\partial y} &= \frac{\partial \tau_{xx}}{\partial x} + \frac{\partial \tau_{xy}}{\partial y} \\ \frac{\partial \rho v_y}{\partial t} + \frac{\partial \rho v_x v_y}{\partial x} + \frac{\partial(\rho v_y^2 + p)}{\partial y} &= \frac{\partial \tau_{xy}}{\partial x} + \frac{\partial \tau_{yy}}{\partial y} \end{aligned} \quad (1)$$

where v_x and v_y are velocity components in x and y coordinates; ρ is the density; t is physical time; and $\tau_{ij} = \mu(v_{i,j} + v_{j,i})$ is stress tensor and μ is the kinematic viscosity.

To solve the incompressible flows numerically, the most challenging task is how to overcome the pressure–velocity coupling. By adding artificial compressibility terms, the governing equations can ensure their hyperbolic properties. And the pseudo-time derivatives are presented in Eq. (1). Hence, the augmented governing equations become

$$\begin{aligned} \frac{1}{\beta_p} \frac{\partial p}{\partial \tau} + \frac{\partial v_x}{\partial x} + \frac{\partial v_y}{\partial y} &= 0 \\ \frac{\partial \rho v_x}{\partial \tau} + \frac{\partial \rho v_x}{\partial t} + \frac{\partial(\rho v_x^2 + p)}{\partial x} + \frac{\partial \rho v_x v_y}{\partial y} &= \frac{\partial \tau_{xx}}{\partial x} + \frac{\partial \tau_{xy}}{\partial y} \\ \frac{\partial \rho v_y}{\partial \tau} + \frac{\partial \rho v_y}{\partial t} + \frac{\partial \rho v_x v_y}{\partial x} + \frac{\partial(\rho v_y^2 + p)}{\partial y} &= \frac{\partial \tau_{xy}}{\partial x} + \frac{\partial \tau_{yy}}{\partial y} \end{aligned} \quad (2)$$

where coefficient β_p is the artificial compressibility, which represents the artificial sound speed. To guarantee the convergence in overall iterative procedure, the value of β_p should be chosen carefully [18].

According to the pseudo time, it is clear that the augmented governing equations with pressure and moment components exhibit hyperbolic properties. For unsteady flows, dual time stepping technique is applied in GSM.

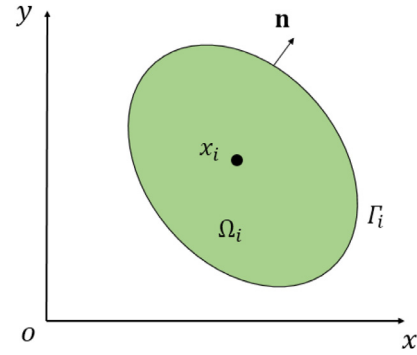


Fig. 1. Smoothing domain for an arbitrary point x_i .

3. Numerical method

3.1. Gradient smoothing operation

The general expression of the gradient at arbitrary location is given in the form of [17]

$$\nabla U_i \equiv \nabla U(x_i) \approx \int_{\Omega_i} \nabla U(x) \hat{\omega}(x - x_i) d\Omega_i \quad (3)$$

By integrating Eq. (3) by part and using divergence theorem, it becomes

$$\nabla U(x_i) \approx \int_{\Gamma_i} U(x) \hat{\omega}(x - x_i) \mathbf{n} d\Gamma_i - \int_{\Omega_i} U(x) \hat{\omega}(x - x_i) d\Omega_i \quad (4)$$

where ∇ is the gradient operator; U is the field variable; x_i is Cartesian coordinate in computational domain; $\hat{\omega}$ is the smoothing function; Ω_i is the gradient smoothing domain; Γ_i is the boundary of Ω_i ; and \mathbf{n} represents the unit normal vector on Γ_i , as shown in Fig. 1.

The smoothing functions in our study can be designed to be piecewise constant as follow:

$$\hat{\omega}(x - x_i) = \begin{cases} 1/A_i, & x \in \Omega_i \\ 0, & x \notin \Omega_i \end{cases} \quad (5)$$

where A_i represents the area of smoothing domain. Substitute Eq. (5) into Eq. (4), it can be simplified as

$$\nabla U(x_i) \approx \frac{1}{A_i} \int_{\Gamma_i} U(x) \mathbf{n} d\Gamma_i \quad (6)$$

Similar with first order derivative, the second order derivative can be further approximated by successfully using gradient smoothing operation.

$$\nabla \cdot (\nabla U_i) \approx \frac{1}{A_i} \int_{\Gamma_i} (\nabla U) \mathbf{n} d\Gamma_i \quad (7)$$

In conclusion, the first and second order derivative of a field variables can be obtained over smoothing domain according to Eqs. (6) and (7). In computational domain, the triangular background cells are generated. The storage location of variables is the vertexes of background grids. Based on the location of interested points, three types of corresponding gradient smoothing domains in GSM are developed. The constructions of the node-associated GSD (nGSD), centroid-associated GSD (cGSD) and midpoint-associated GSD (mGSD) [17] are illustrated in Fig. 2.

3.2. Discretization of governing equations

3.2.1. Semi-discretized governing equations

The conservative vector form of incompressible Navier–Stokes equations can be expressed as

$$\mathbf{P} \frac{\partial \mathbf{Q}}{\partial \tau} + \frac{\partial \mathbf{U}}{\partial t} + \nabla \cdot (\mathbf{F}_c - \mathbf{F}_v) = 0 \quad (8)$$

Download English Version:

<https://daneshyari.com/en/article/6924921>

Download Persian Version:

<https://daneshyari.com/article/6924921>

[Daneshyari.com](https://daneshyari.com)